SPATIALLY-RESOLVED DOPANT CHARACTERIZATION WITH A SCANNING MICROWAVE MICROSCOPE*

T. Mitch Wallis, Atif Imtiaz, Alexandra E. Curtin, Pavel Kabos, Matthew D. Brubaker, Norman A. Sanford, and Kris A. Bertness

National Institute of Standards and Technology (NIST), 325 Broadway, Boulder, Colorado 80305

INTRODUCTION

The scanning microwave microscope (SMM) is a tool for spatially-resolved microwave characterization of nanoelectronic materials and devices. The microscope incorporates a sharp, near-field probe, which measures local changes in reflected microwave signals from a device under test (DUT). With proper calibration and modeling, a variety of parameters can be extracted from the measurements, including impedance,[1] absolute capacitance,[2,3] and dopant concentration.[4,5] Here, we describe two additional capabilities of the SMM related to dopant profiling. First, we discuss the capability to tune the contrast in $d(S_{11})/dV$ images of variably-doped samples by adjusting the SMM operating frequency. Second, we demonstrate capabilities to locate a p-n junction within a GaN nanowire (NW) and observe changes in the junction morphology as a function of applied SMM bias.

The commercial SMM used in these experiments is illustrated in Fig. 1(a) and described elsewhere.[2] The SMM incorporates a broadband (DC to 18 GHz) signal path with an atomic force microscope (AFM), effectively forming a one-port microwave network in which the DUT acts as a load. With the AFM operating in contact mode, the complex scattering parameter for the reflected microwave signal, S_{11}, is measured by use of a vector network analyzer. Thus, the system simultaneously acquires topographic data along with images of S_{11}. Additionally, by applying a small, low-frequency modulation bias to the SMM probe, a lockin technique can be used to extract the derivative $d(S_{11})/dV$, which is proportional to the absolute capacitance.[2] In addition to the modulation bias, a variable DC bias (V) may be applied to the probe tip, allowing for measurement of the dC/dV versus V curve. In turn, measurements of the voltage dependence of dC/dV enable quantitative determination of dopant concentration.[4]

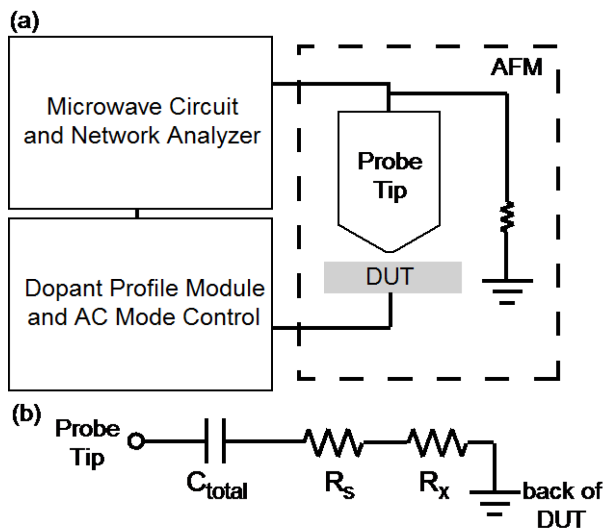

FIGURE 1. (a) Simplified schematic of the commercial SMM (b) Simple circuit used to model probe-DUT interactions. Both figures based on Reference 7.

FREQUENCY-DEPENDENT SENSITIVITY OF SMM

SMM measurements can be used to extract calibrated, spatially-resolved dopant profiles.[4] Such measurements require well-characterized reference samples with regions of known dopant densities. Here, we measured samples produced by the IMEC Center for Advanced Metrology Solutions.[6] The samples are p-type doped Si, topography-free and comprise a series of parallel dopant density regions with densities varying in decade increments (10^{16} cm^{-3}, 10^{17} cm^{-3}, 10^{18} cm^{-3}, and so on). Each region is a stripe about 1.5 μm wide and many mm long.

In Fig. 2, $d(S_{11})/dV$ images of the reference sample are shown at three operating frequencies: 2.20 GHz, 13.37 GHz, and 17.86 GHz. Regions of constant dopant density run vertically through the image as indicated by dashed lines in Fig. 2. The DC SMM bias was adjusted from 0.00 V to -3.00 V during image acquisition. Beginning at the topmost horizontal scan lines, the data was acquired with a bias of 0.00 V. Throughout the scan, the bias was adjusted sequentially until the bias was -3.00 V in the bottommost scan lines. In the 2.20 GHz image, maximum contrast is observed in the 10^{16} cm^{-3} and 10^{17} cm^{-3} stripes. In the 13.37 GHz image, the contrast is altered, though both the 10^{16} cm^{-3} and 10^{17} cm^{-3} stripes still show significant contrast. Finally, in the 17.86 GHz image, maximum contrast is confined to the 10^{17} cm^{-3} stripe.

One simple approach to understanding the frequency-dependent contrast is to model the path from probe to ground with a lumped element circuit, shown in Fig. 1(b).[7] The total capacitance, C_{total}, is a series combination of the depletion layer capacitance, C_D, and the oxide capacitance, C_{ox}. C_D is calculated via a standard MOS model, with the probe tip acting as the metal, the Si acting as the semiconductor, and the Si oxide in between. R_s is the local sheet resistance and R_x is the resistance of the Si sample between the local region under the probe and the ground connection. Both C_{total} and R_s depend on local dopant density. Thus, for a given dopant density, a selection frequency $(\tau_{sel})^{-1}$ may be calculated from $\tau_{sel} = \xi(Rs + Rx)\ C_{total}$, where ξ is a dimensionless factor that depends on probe geometry. The existence of a selection frequency for each dopant density enables the SMM to enhance sensitivity and image contrast by an adjustment of operating frequency.

IMAGING P-N JUNCTIONS

In addition to the SMM's frequency-dependent sensitivity to the magnitude of the dopant density, the SMM is also capable of locating p-n junctions within a device. In order to demonstrate this, we imaged axial p-n junction GaN NWs with the

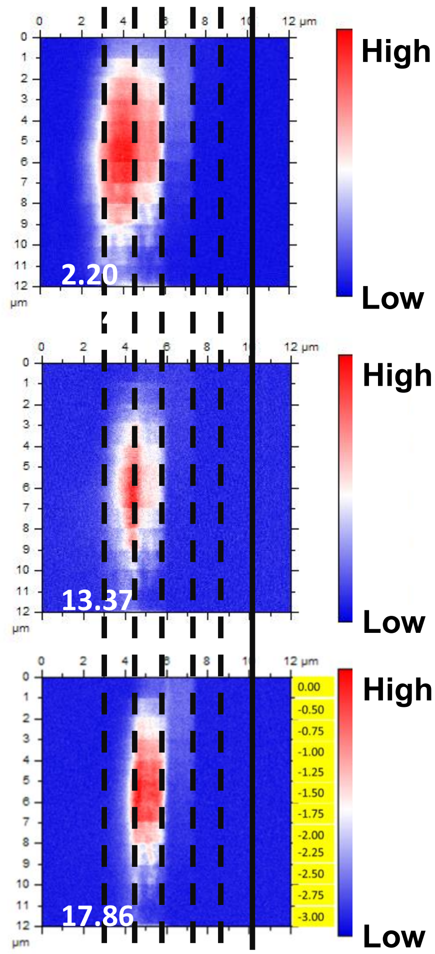

FIGURE 2. d(S11)/dV images of the variably doped Si sample taken at SMM operating frequencies of 2.20 GHz, 13.37 GHz, and 17.86 GHz. Vertical dashed lines indicate boundaries between differently doped regions. Solid line indicates sample edge. DC probe bias sequence indicated at the right side of the 17.86 GHz image.

SMM. The GaN NWs were synthesized by plasma-assisted molecular beam epitaxy and doped *in-situ* during growth to produce axial p-n junctions.[8] The thinner NW root was doped p-type, for approximately 40% of the overall growth duration and the thicker NW tip was doped n-type. Single NWs produce diode-like I-V characteristics, although the individual p-sections exhibited low conductivity.

Fig. 3 shows images of GaN NWs dispersed on SiO_x / Si. The topography image is consistent with other studies of these NWs, displaying maximum

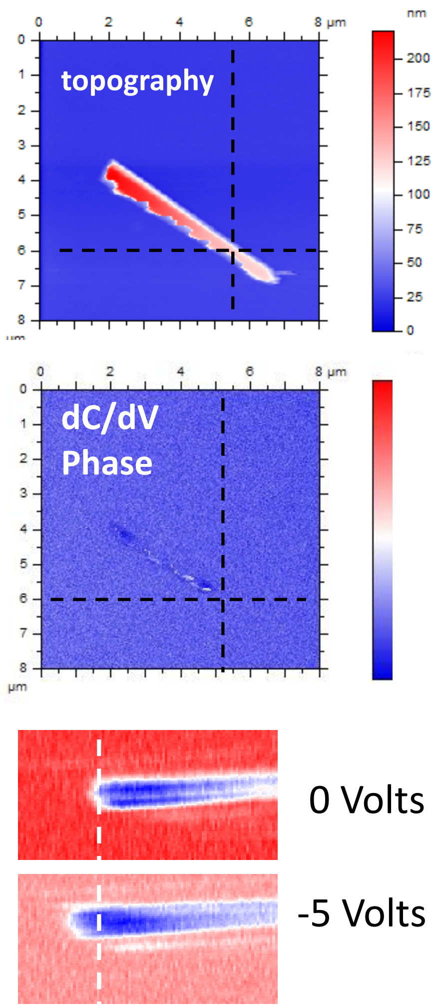

FIGURE 3. (Top) Contact AFM topography of GaN NW (12 μm X 12 μm). (Middle) *dC/dV* phase image, operating frequency 18.5 GHz. (Bottom) *dC/dV* amplitude images of p-n junction at 0 Volts and -5 Volts. Note that the color scale is reversed in the bottom panel.

apparent diameter on the order of 200 nm and a gradual taper in the diameter over the length of the wire. The apparent length of the structure is about 6 μm. However, the apparent length decreases to about 4 μm in simultaneously acquired *dC/dV* amplitude and phase images (phase image shown in Fig. 3, middle panel). In other words, only the n-type segment of the NW shows a response in the *dC/dV* images. To study bias-dependent morphology of the p-n junction, additional NWs were dispersed on a TiAl metal layer supported by SiO_x / Si. In the bottom panel of Fig. 3, the apparent length of the n-type segment increases by about 200 nm when a bias of -5 V is applied to the SMM probe. While a full theory of these phenomena is still under development, it is clear that SMM is capable of locating p-n junctions in devices and enables bias-dependent study of the morphology of such junctions.

REFERENCES

* Contribution of an agency of the U.S. government; not subject to copyright.

1. M. Farina, D. Mencarelli, A. Di Donato, G. Venanzoni, and A. Morini, *IEEE Trans. Microwave Theory and Techn.* **59**, 2769-2776 (2011).
2. H. P. Huber, *et. al.*, *Rev. Sci. Instrum.* **81**, 113701 (2010).
3. A. Karbassi, *et. al.*, *Rev. Sci. Instrum.* **79**, 094706 (2008).
4. H. P. Huber, *et. al.*, *J. of Applied Phys.* **111**, 014301 (2012).
5. J. J. Kopanski, J. F. Marchiando, and J. R. Lowney, *Mater. Sci. Eng. B-Solid State Mater. Adv. Tech.* **44**, 46 (1997).
6. Trade names are used to provide clarity and do not imply endorsement by NIST or the U.S. government.
7. A. Imtiaz, *et. al. J. of Applied Phys.* **111**, 093727 (2012).
8. K. A. Bertness, A. Roshko, N. A. Sanford, J. M. Barker, and A. V. Davydov, *J. of Crystal Growth* **287**, 522 (2006).

KEYWORDS

Dopant profiling, Nanoelectronics, p-n junctions, Scanning microwave microscopy